Effect of Al Substitution on the Electronic and Magnetic Properties of $GdCo_5$

A. Szajek* and W.L. Malinowski

Institute of Molecular Physics, Polish Academy of Sciences
Smoluchowskiego 17, 60-179 Poznań, Poland

(Received September 19, 2001; revised version February 7, 2002)

Experimental data show that aluminium doped RCo_5 systems crystallize in $CaCu_5$-type structure for most of the rare-earth elements (R). Al impurities randomly occupy one of the two possible positions (2c and 3g) and there is a critical concentration of Al, $x_c = 2.0$, for $RCo_{5-x}Al_x$ when the Co sublattice becomes nonmagnetic. The *ab initio* self-consistent calculations show strong dependence of magnetic properties of $GdCo_{5-x}Al_x$ on concentration of Al and position of the impurities in the unit cell, furthermore to fulfil experimental observation of existence of critical concentration, $x_c = 2.0$, the Al impurities should prefer 3g positions otherwise the magnetic moments on Co atoms do not vanish.

PACS numbers: 71.20.–b, 71.20.Eh

1. Introduction

Intermetallic compounds of rare-earth (R) atoms and transition-metal (T) atoms are of great importance both for the technological applications and from fundamental physical point of view. First, the strongest permanent magnets belong to this class of materials and some of them are promising materials for use in batteries because of their special electrochemical properties. Second, they represent a big challenge for the electron theory because their properties are determined by two different types of electronic states, i.e. the highly correlated and strongly

*corresponding author; e-mail: szajek@ifmpan.poznan.pl

localized $4f$ states of rare-earth atoms and the valence states of transition-metal atoms which are comparatively weakly correlated and more delocalized.

Generally, in the R–T compounds, there are three types of exchange interactions: T–T interactions between magnetic moments of the T sublattice, the R–T intersublattice interactions and the R–R interactions between the magnetic moments within the R sublattice. These interactions lead to the R($5d$)–T($3d$) hybridization. Introduction of a metalloid (M = B, Al or Ga) to the R–T system causes additional hybridization T($3d$)–M(p) and R($5d$)–M(p).

$R(T_{1-x}M_x)_5$ is a one of the most intensively examined systems, where R is rare-earth metal, T = Co or Ni, and M = B, Al or Ga. The initial RT_5 system has hexagonal ($P6/mmm$) $CaCu_5$-type structure having two inequivalent positions of T atoms: 2c and 3g (see Fig. 1). Especially intensively examined were $R(Co_{1-x}B_x)_5$ because they form an interesting series of crystal structures (see [1] and references therein) which can be expressed by a general formula $R_{n+1}Co_{3n+5}B_{2n}$ (n = 0, 1, 2,..., ∞). Although the systems have uniaxial symmetry, their Curie temperatures and saturation magnetization are too low to be suitable for permanent magnet applications [2–4]. In order to overcome this drawback new series of compounds $R_{m+1}Co_{5m+3}B_2$ with high Co content was proposed [5–8]. The mentioned above two homologous series can be expressed by a generalized formula $R_{m+n}Co_{5m+3n}B_{2n}$, which is formed by alternative stacking of m parts of RCo_5 with n parts of RCo_3B_2 along the c axis.

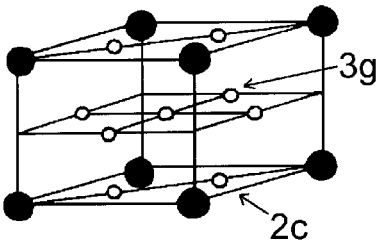

Fig. 1. $CaCu_5$-type unit cell. Small circles describe Co and Al atoms occupying 2c and 3g positions. La atoms occupy 1a positions described by large circles.

$La(Ni_{1-x}(Al,Co)_x)_5$ systems and their hydrides were examined as potential materials for batteries. Hydrogen storage alloys based on La are commercially used as negative electrode materials for nickel–metal hydride (Ni–MH_x) battery [9–12]. These materials combine a high reversible energy storage capacity with fast electrochemical activation, excellent long-term cycling stability and good charge/discharge kinetics. In these alloys the initial $CaCu_5$-type structure is conserved and the neutron diffraction measurements as well as the total energy *ab initio* calculations [13–15] showed that Al and Co impurities prefer the 3g positions. Similar results were also obtained for $LaNi_{5-x}T_x$ (T = Fe or Mn) [16, 17].

The X-ray analysis revealed that also $R(Co_{1-x}Al_x)_5$ alloys with $x < 0.3$ are single phase, occur in the $CaCu_5$ structure, and the intensities of the X-ray lines showed that Al atoms randomly occupy the Co sites. Al substitutions for Co in RCo_5 brings three important effects on the magnetic properties of RCo_5 [18]: a decrease in the Curie temperature (T_C) and magnetic moments of Co atoms (μ_{Co}), and a change of magnetic anisotropy. The T_C and μ_{Co} vanish at a critical concentration of Al, $x_c = 0.4$. Similar situation is for RCo_3B_2.

The aim of this paper is to investigate relation between different positions of Co and Al atoms in $Gd(Co_{1-x}Al_x)_5$ systems ($x = 0$, 0.2, and 0.4) and their magnetic properties based on the spin polarized *ab initio* calculations.

2. Computational method

The electronic structure was calculated based on the tight-binding linear muffin-tin orbital (TB LMTO) method in the atomic sphere approximation (ASA) [19, 20]. In the ASA the unit cell is filled by Wigner–Seitz spheres having the same total volume: $(4\pi/3)\sum_j S_j^3 = N(4\pi/3)S_{av}^3 = V$, where j ($j = 1, \ldots N$) is the index of atom in the unit cell, N is number of atoms in the cell, S_j is the Wigner–Seitz radius of the j-th atom, S_{av} is the average Wigner–Seitz radius, V is the volume of the unit cell. In our case the unit cell contains one formula unit ($N = 5$ atoms). The hexagonal unit is presented in Fig. 1.

The coordinates of the atoms in the unit cell were taken from [6] and are summarized in Table I. The overlap volume of the muffin-tin spheres is about 8.2%. The standard combined correction terms [19] for overlapping were used to compensate for errors due to the ASA. The scalar relativistic approximation for band electrons and the fully relativistic treatment for the frozen core electrons were used. The spin–orbit interactions were taken into account in the form proposed by Min and Jang [21]. The exchange correlation potential was assumed in the form proposed by von Barth and Hedin (BH) [22] and, for comparison, by Perdew et al. (PW) [23] with non-local corrections. The starting atomic configurations were taken as: core + $4f^7 5d^1 6s^2$ for Gd, core + $3d^7 4s^2$ for Co and core + $3s^2 3p^1$ for Al atom. The spin-polarized calculations were performed for the experimental values of the lattice constants [18] and for all possible positions of Al impurities in the unit cell. In the case of $GdCo_4Al$ the single Al atoms are located in 3g and 2c positions one after another. For $GdCo_3Al_2$ the situation is more complicated and all possible configurations were considered: two Al atoms in 2c or 3g positions, and a mixed situation, where the impurities are located in 2c and 3g sites. The crystallographic characteristics are collected in Table I. The self-consistent calculations were performed for at least 9248 k-points in the whole Brillouin zone. The number of k-points was dependent on the symmetry of considered systems, determined by positions of Al impurities in the unit cell. The tetrahedron method [24–26] was used for integration over the Brillouin zone. The iterations were repeated until the

TABLE I

Crystallographic characteristics of $GdCo_5$, $GdCo_4Al$, and $GdCo_3Al_2$ compounds: the lattice constants a and c, the Wigner–Seitz radii (in a.u., average, S_{av}, and for particular atoms). The lattice constants for $GdCo_3Al_2$ were extrapolated from experimental data for smaller concentrations of Al.

Positions and [coordinates] of atoms	Lattice constants and Wigner–Seitz radii used in calculations					
	$GdCo_5$	$GdCo_4Al$		$GdCo_3Al_2$		
	$a = 9.39950$	$a = 9.49399$		$a = 9.59520$		
	$c = 7.52678$	$c = 7.60993$		$c = 7.69788$		
	$S_{av} = 2.84034$	$S_{av} = 2.86983$		$S_{av} = 2.90128$		
3g-1	Co	Al	Co	Al	Al	Co
[1/2, 1/2, 1/2]	2.6463	2.6965	2.6527	2.7264	2.7053	2.6818
3g-2	Co	Co	Co	Al	Co	Co
[1/2, 0, 1/2]	2.6463	2.6965	2.6527	2.7264	2.7053	2.6818
3g-3	Co	Co	Co	Co	Co	Co
[0, 1/2, 1/2]	2.6463	2.6965	2.6527	2.7264	2.7053	2.6818
2c-1	Co	Co	Al	Co	Al	Al
[2/3, 1/3, 0]	2.6518	2.6320	2.7285	2.6632	2.7107	2.7611
2c-2	Co	Co	Co	Co	Co	Al
[1/3,2/3,0]	2.6518	2.6320	2.7285	2.6632	2.7107	2.7611
1a	Gd	Gd	Gd	Gd	Gd	Gd
[0, 0, 0]	3.5457	3.5966	3.5617	3.6331	3.6164	3.5976

energy eigenvalues of the consecutive iteration steps were the same within an error 0.01 mRy.

3. Results and discussion

The TB LMTO ASA method allows differentation of the ions in the cell but effect of disorder due to Al substitution is neglected. In the case of the Haucke-type phase $GdCo_5$ (see Fig. 1 and Table I), two types of Co sites must be distinguished: the 2-fold degenerate basal sites (2c) located in the basal plane together with Gd atoms and 3-fold degenerate non-basal sites (3g) located in the plane with $z = 1/2$. In accordance with experimental observations for $LaNi_5$ [27] and $GdCo_5$ [18], it is assumed that the Gd sites do not accommodate Co and Al atoms. The total densities of states (DOS) and local contributions of individual atoms are presented in Figs. 2–7. The electronic structure of $GdCo_5$ was calculated earlier by other authors [28, 29]. These calculations were performed using different methods but they are consistent with ours. Therefore we treat our calculations for this system as reference results for the doped compounds to avoid discussion on differences which can be caused by distinct approaches and technical details.

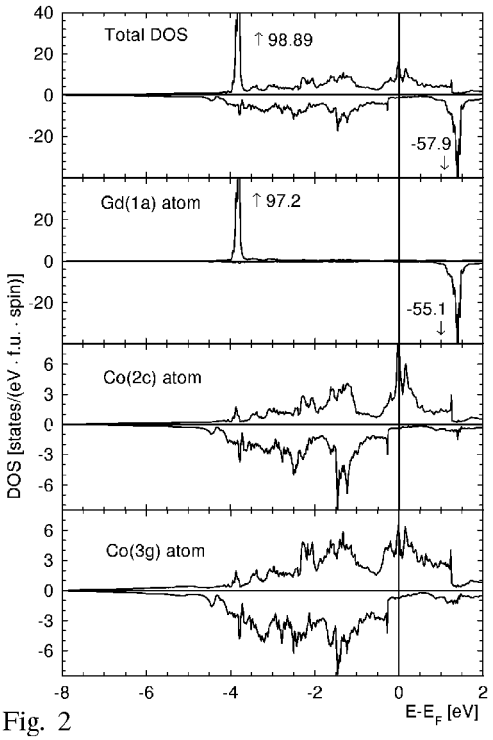

Fig. 2

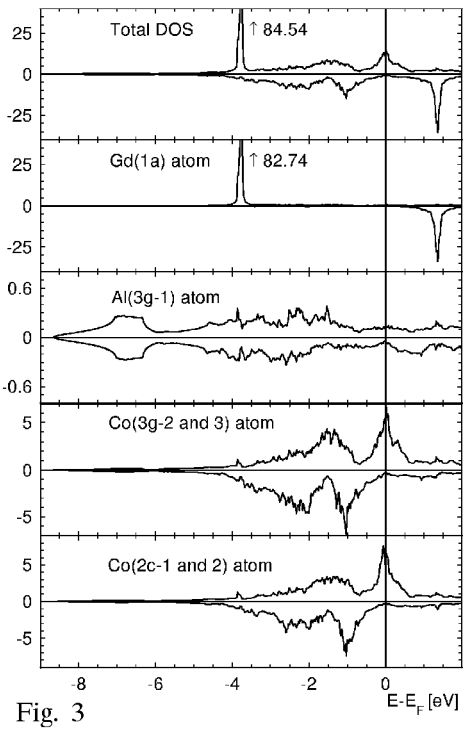

Fig. 3

Fig. 2. The total and site-projected DOS functions for the $GdCo_5$ compound.
Fig. 3. The total and site-projected DOS functions for the $GdCo_4Al$ compound for Al located in 3g-1 position.

The width of the valence band of the $GdCo_5$ system is about 7.9 eV. The valence bands for $GdCo_4Al$ and $GdCo_3Al_2$ are wider, by about 0.8 and 1.3 eV, respectively. It is caused by the Al atoms, their s and p electrons are located near the bottom of the valence band. The valence bands of the doped systems are wider than for the undoped case and because of reduced number of valence electrons (see Table II) the values of DOS at the Fermi level should also be lower.

It is generally true but strongly depends on the location of the Al impurities (see Table III).

The impurities cause charge transfer between ions: from Al to Co and Gd atoms. Electron transfer to Co atoms fulfils d band and reduces their magnetic moments (see Table IV).

The Al atoms cause reconstruction of the starting $GdCo_5$ band structure and change the values of DOS at the Fermi level. The DOS($E = E_F$) for $GdCo_5$ is equal to about 15.81 states/(eV f.u.) with about 95% contribution of Co atoms (2.318 and 4.04 states/(eV atom) for Co(3g) and Co(2c) atoms, respectively).

For $GdCo_4Al$ systems the values of DOS(E_F) decrease and reach 12.036 and 8.554 states/(eV f.u.) for impurities located in 3g and 2c sites, respectively. In both

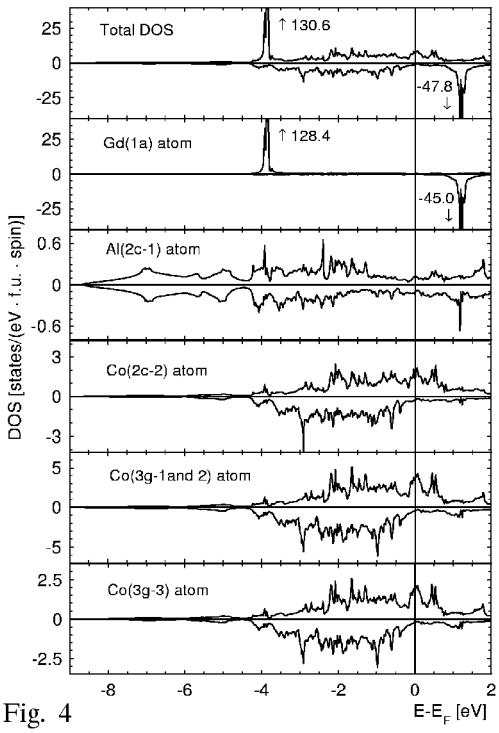

Fig. 4

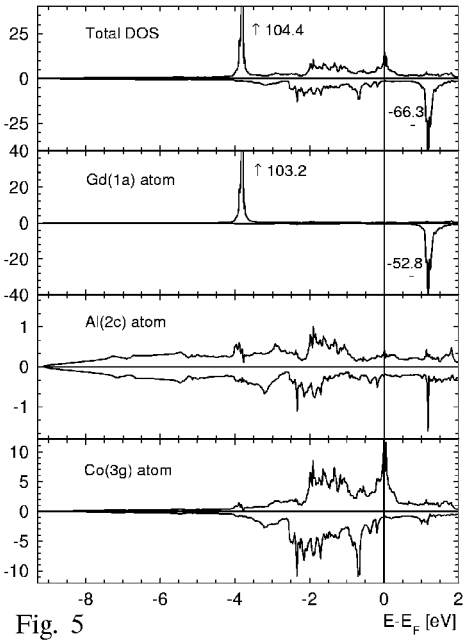

Fig. 5

Fig. 4. The total and site-projected DOS functions for the $GdCo_4Al$ compound for Al atom located in 2c-1 position.

Fig. 5. The total and site-projected DOS functions for the $GdCo_3Al_2$ compound for two atoms of Al located in 2c positions. The Fermi level is located in the high peak of DOS formed by the Co(d) electrons. In this configuration the DOS($E = E_F$) and the magnetic moments on Co atoms reach the highest values (see Table III and IV).

cases the highest values of magnetic moments for Co atoms were obtained in nearest neighbouring of Al atoms. Similar phenomenon was observed for $R(Co_{1-x}Al_x)_2$ (R = rare-earth or yttrium atom), where small concentrations (about 10%) of Al atoms increase the Curie temperatures of these compounds [30]. In the case of $GdCo_{4.5}Al_{0.5}$ the mean magnetic moment for Co is higher than for undoped system [18, 31].

For the $GdCo_4Al$ system and the BH potential the calculated mean magnetic moments for Co atoms are equal to 1.053 and 1.122 μ_B/Co atom for Al atoms located in 3g and 2c sites, respectively. The second value is closer to the experimental result, which varies from 1.25 to 1.43μ_B [18, 31, 32]. Similarly is for the calculations with the PW potential but the values are slightly higher: 1.140 and 1.202 μ_B/Co atom, respectively. Small magnetic moments, about 0.1 μ_B/atom, parallel oriented to the Gd ones, are induced on Al atoms. The moments on Co atoms have opposite directions to the moments located on Gd ones. The differ-

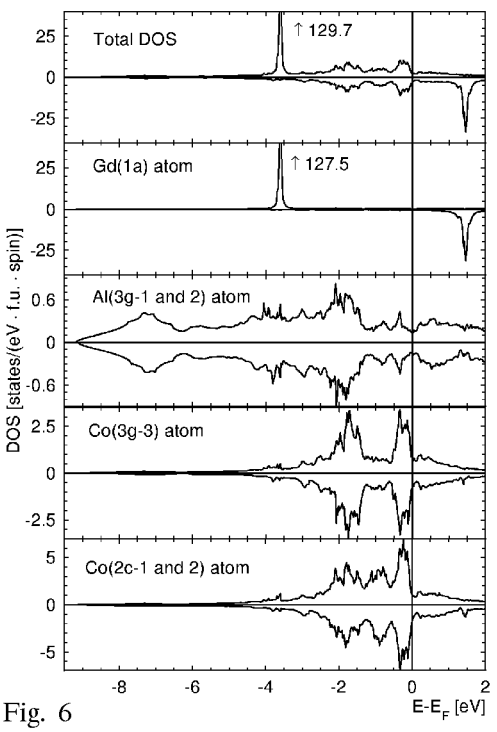

Fig. 6

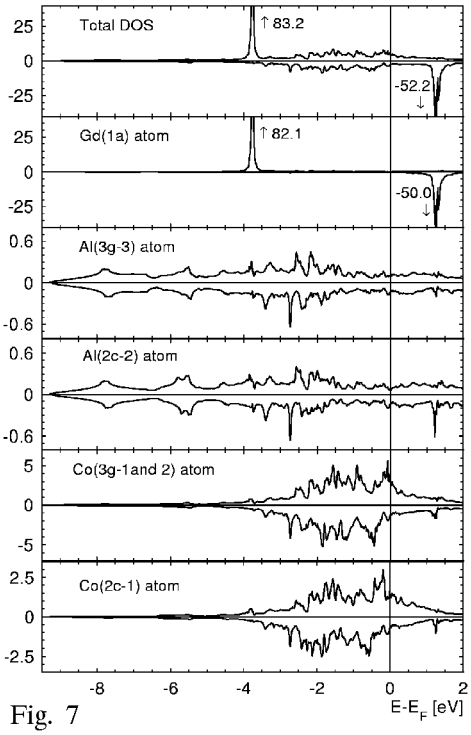

Fig. 7

Fig. 6. The total and site-projected DOS functions for the $GdCo_3Al_2$ compound for two atoms of Al located in 3g-1 and 3g-2 positions. The Fermi level is located above the peaks formed by Co(d) electrons. The values of DOS($E = E_F$) reach the lowest values and the magnetic moments on Co atoms are close to zero.

Fig. 7. The total and site-projected DOS functions for the $GdCo_3Al_2$ compound for two atoms of Al located in 3g-3 and 2c-2 positions. An intermediate situation to the presented in Figs. 5 and 6. The Co magnetic moments reach the values of about 0.4–0.5 μ_B/atom.

ences between mean magnetic moments for distinct localizations of Al atoms are very small (0.087 and 0.080 μ_B/Co atom for BH and PW potentials, respectively) and it is very difficult to admit them as conclusive for site preference of the impurities. Detailed analysis of X-ray diffraction patterns for YCo_4Al and $NdCo_4Al$ systems [33] showed that distribution of Al on the 3g and 2c sites of $CaCu_5$-type structure is not quite random. The Al atoms prefer a little more the 3g site than the 2c one. However, for light rare-earth metals situation can be slightly different because of $4f$–$3d$ hybridization. The obtained rare-earth moments (for Nd, Pr, and Sm atoms) were considerably smaller than the free trivalent ion values. This discrepancy increases with increasing concentration of Al atoms and displays important role of Al($3p$) electrons in hybridization effects.

Second Co atom replaced by Al one in $GdCo_4Al$ intensifies the decrease in

TABLE II

Total numbers of valence electrons (NOS; per f.u.) and individual contributions of the Gd, Co, and Al atoms to the electron count in the $GdCo_5$, $GdCo_4Al$, and $GdCo_3Al_2$ compounds. The starting occupation numbers were the following: Gd($4f^7 5d^1 6s^2$), Co($3d^7 4s^2$), and Al($3s^2 3p^1$).

Positions of atoms	Number of electrons per atom					
	$GdCo_5$	$GdCo_4Al$		$GdCo_3Al_2$		
	Total NOS					
	55	49		43		
3g-1	Co	Al	Co	Al	Al	Co
	s 0.688	*s* 0.953	*s* 0.665	*s* 0.955	*s* 0.931	*s* 0.656
	p 0.708	*p* 1.299	*p* 0.727	*p* 1.359	*p* 1.358	*p* 0.784
	d 7.560	*d* 0.315	*d* 7.611	*d* 0.312	*d* 0.302	*d* 7.669
3g-2	Co	Co	Co	Al	Co	Co
	s 0.6828	*s* 0.696	*s* 0.665	*s* 0.955	*s* 0.672	*s* 0.657
	p 0.7076	*p* 0.763	*p* 0.727	*p* 1.359	*p* 0.773	*p* 0.780
	d 7.5596	*d* 7.633	*d* 7.611	*d* 0.312	*d* 7.712	*d* 7.669
3g-3	Co	Co	Co	Co	Co	Co
	s 0.688	*s* 0.696	*s* 0.665	*s* 0.694	*s* 0.672	*s* 0.657
	p 0.708	*p* 0.763	*p* 0.727	*p* 0.772	*p* 0.773	*p* 0.780
	d 7.560	*d* 7.633	*d* 7.611	*d* 7.722	*d* 7.712	*d* 7.669
2c-1	Co	Co	Al	Co	Al	Al
	s 0.664	*s* 0.633	*s* 0.964	*s* 0.626	*s* 0.945	*s* 0.968
	p 0.647	*p* 0.622	*p* 1.254	*p* 0.634	*p* 1.272	*p* 1.290
	d 7.585	*d* 7.633	*d* 0.330	*d* 7.742	*d* 0.290	*d* 0.345
2c-2	Co	Co	Co	Co	Co	Al
	s 0.664	*s* 0.633	*s* 0.705	*s* 0.626	*s* 0.669	*s* 0.968
	p 0.647	*p* 0.622	*p* 0.718	*p* 0.634	*p* 0.698	*p* 1.290
	d 7.585	*d* 7.633	*d* 7.656	*d* 7.742	*d* 7.701	*d* 0.345
1a	Gd	Gd	Gd	Gd	Gd	Gd
	s 0.591	*s* 0.616	*s* 0.586	*s* 0.617	*s* 0.602	*s* 0.596
	p 0.725	*p* 0.755	*p* 0.724	*p* 0.785	*p* 0.765	*p* 0.746
	d 1.724	*d* 1.766	*d* 1.766	*d* 1.792	*d* 1.833	*d* 1.830
	f 7.300	*f* 7.336	*f* 7.289	*f* 7.362	*f* 7.320	*f* 7.291

DOS($E = E_F$) but only in the case when at least one of the Al atoms is located in 3g site: 5.159 states/(eV f.u.) for two Al atoms in 3g sites and 7.486 states/(eV f.u.) for impurities simultaneously located in 3g and 2c sites. The magnetic moments on Co atoms are reduced. Especially in the first case where mean magnetic moment on Co atoms is equal to 0.028 μ_B/atom, and Co moments located in 2c sites are parallel to the moments of Gd atoms.

TABLE III

The values of the spin projected DOS at the Fermi level for the $GdCo_5$, $GdCo_4Al$, and $GdCo_3Al_2$ compounds. The upper values concern the electrons with spin up and the lower ones the electrons with opposite spin direction (total DOS calculated per f.u.).

Positions of atoms	DOS [states/(eV spin atom)]					
	$GdCo_5$	$GdCo_4Al$		$GdCo_3Al_2$		
	Total DOS					
	14.290	11.295	7.341	2.202	5.022	13.051
	1.520	0.741	1.213	2.957	2.464	1.489
	Co	Al	Co	Al	Al	Co
3g-1	2.052	0.116	1.863	0.072	0.102	4.134
	0.266	0.055	0.206	0.077	0.124	0.331
	Co	Co	Co	Al	Co	Co
3g-2	2.052	2.794	1.863	0.072	1.617	4.134
	0.266	0.148	0.206	0.077	0.608	0.331
	Co	Co	Co	Co	Co	Co
3g-3	2.052	2.794	1.863	0.771	1.617	4.134
	0.266	0.148	0.206	0.740	0.608	0.331
	Co	Co	Al	Co	Al	Al
2c-1	3.832	2.575	0.130	0.541	0.074	0.190
	0.208	0.134	0.103	0.880	0.131	0.106
	Co	Co	Co	Co	Co	Al
2c-2	3.832	2.575	1.389	0.541	1.389	0.190
	0.208	0.134	0.255	0.880	0.661	0.106
	Gd	Gd	Gd	Gd	Gd	Gd
1a	0.470	0.441	0.233	0.205	0.223	0.269
	0.306	0.122	0.237	0.303	0.332	0.284

In the rest of the considered configurations Co moments are always antiparallel oriented to the Gd ones. The magnetic moments induced on Al atoms in this configuration reach the smallest values ($\approx 10^{-3}\ \mu_B$/atom). In the second case (two Al atoms simultaneously in 2c and 3g sites) the Co magnetic moments are larger and reach values $0.4 \div 0.5\ \mu_B$/atom (see Table IV). These values seem to be too high comparing with experimental measurements [18] which show that the Co moments should have values close to zero. Similar conclusion is for the case where two Al atoms are located in 2c sites. DOS(E_F) reaches the highest value 14.54 states/(eV f.u.) and the Co magnetic moments are above $0.7\ \mu_B$/atom.

TABLE IV

The *ab initio* calculated total (in μ_B per f.u.) and local magnetic moments (in μ_B per atom) for $GdCo_{5-x}Al_x$, $x = 0$, 1.0 and 2.0, when the Al impurities are located in different crystallographic positions. The calculations were performed for two types of the exchange-correlation potential: BH and PW (the values in parenthesis).

Positions of atoms	Magnetic moments [μ_B/(f.u. or atom)]					
	$GdCo_5$	$GdCo_4Al$		$GdCo_3Al_2$		
	–0.038	–3.027	–2.809	–7.069	–5.824	–5.000
	(–0.188)	(–2.819)	(–2.636)	(–6.964)	(–5.169)	(–4.684)
3g-1	Co 1.440	Al –0.073	Co 1.091	Al 0.003	Al –0.017	Co 0.727
	(1.514)	(–0.104)	(1.170)	(–0.001)	(–0.040)	(0.883)
3g-2	Co 1.440	Co 1.098	Co 1.091	Al 0.003	Co 0.384	Co 0.727
	(1.514)	(1.191)	(1.170)	(–0.001)	(0.660)	(0.883)
3g-3	Co 1.440	Co 1.098	Co 1.091	Co 0.049	Co 0.384	Co 0.727
	(1.514)	(1.191)	(1.170)	(0.152)	(0.660)	(0.883)
2c-1	Co 1.456	Co 1.007	Al –0.082	Co –0.066	Al –0.035	Al –0.041
	(1.517)	(1.089)	(–0.116)	(–0.035)	(–0.064)	(–0.067)
2c-2	Co 1.456	Co 1.007	Co 1.214	Co –0.066	Co 0.524	Al –0.041
	(1.517)	(1.089)	(1.298)	(–0.035)	(0.797)	(–0.067)
1a	Gd –7.270	Gd –7.164	Gd –7.214	Gd –6.992	Gd –7.064	Gd –7.099
	(–7.388)	(–7.275)	(–7.328)	(–7.044)	(–7.182)	(–7.199)

4. Conclusions

A systematic study of magnetic moments of $GdCo_5$, $GdCo_4Al$, and $GdCo_3Al_2$ compounds was performed using TB LMTO ASA method. The calculated results were compared with experimental data [18], which reported existence of a critical concentration of Al, $x_c = 2$, for $GdCo_{5-x}Al_x$ when the Co sublattice becomes nonmagnetic. Our calculations showed strong dependence of magnetic properties of $GdCo_{5-x}Al_x$ on concentration of Al and position of the impurities in the unit cell. To fulfil experimental observation of existence of the critical concentration the Al impurities should prefer 3g sites otherwise the magnetic moments on Co atoms do not vanish.

Acknowledgments

The band calculations were performed in the Supercomputer and Networking Centre in Poznań (PCSS).

References

[1] A. Szajek, *J. Magn. Magn. Mater.* **185,** 322 (1998).

[2] A.T. Pedziwiatr, S.Y. Jiang, W.E. Wallace, E. Burzo, V. Pop, *J. Magn. Magn. Mater.* **66,** 69 (1987).

[3] R. Tetean, E. Burzo, *J. Magn. Magn. Mater.* **157/158,** 633 (1996).

[4] T. Ito, H. Asano, H. Ido, M. Yamada, *J. Appl. Phys.* **79,** 5507 (1996).

[5] Yi Chen, Q.L. Liu, J.K. Liang, X.L. Chen, B.G. Shen, F. Huang, *Appl. Phys. Lett.* **74,** 856 (1999).

[6] Yi Chen, J.K. Liang, X.L. Chen, X.L. Liu, *J. Alloys Comp.* **289,** 96 (1999).

[7] Yi Chen, J.K. Liang, X.L. Chen, Q.L. Liu, B.G. Shen, Y.P. Shen, *J. Phys., Condens. Matter* **11,** 8251 (1999).

[8] Yi Chen, X. Li, L. Chen, J.K. Liang, B.G. Shen, Q.L. Liu, *Phys. Rev. B* **61,** 3502 (2000).

[9] K.H.J. Buschow, P.C.P. Bouten, A.R. Miedema, *Rep. Prog. Phys.* **45,** 937 (1982).

[10] J.J.G. Willems, *Philips J. Res.* **36,** 1 (1984).

[11] L. Schlapbach, in: *Hydrogen in Intermetallic Compounds, II*, Ed. L. Schlapbach, Springer, Berlin 1992, p. 165.

[12] A. Anani, A. Visintin, K. Petrov, S. Srinivasan, J.J. Reilly, J.R. Johnson, R.B. Schwarz, P.B. Desch, *J. Power Sources* **47,** 261 (1994).

[13] J.-M. Joubert, R. Černý, M. Latroche, A. Percheron-Guégan, K. Yvon, *J. Appl. Crystallogr.* **31,** 327 (1998).

[14] J.-M. Joubert, R. Černý, M. Latroche, A. Percheron-Guégan, K. Yvon, *J. Alloys Comp.* **265,** 311 (1998).

[15] A. Szajek, M. Jurczyk, W. Rajewski, *J. Alloys Comp.* **307,** 290 (2000).

[16] C.Y. Tai, G.K. Marasinghe, G.D. Waddill, O.A. Pringle, W.J. James, *J. Appl. Phys.* **87,** 6731 (2000).

[17] J.B. Yang, C.Y. Tai, G.K. Marasinghe, G.D. Waddill, O.A. Pringle, W.J. James, Y. Kong, *Phys. Rev. B* **63,** 014407 (2001).

[18] H. Ido, K. Konno, S.F. Cheng, W.E. Wallace, S.G. Sanker, *J. Appl. Phys.* **67,** 4638 (1990).

[19] O.K. Andersen, O. Jepsen, M. Šob, in: *Electronic Structure and Its Applications*, Ed. M.S. Yussouff, Springer, Berlin 1987, p. 2.

[20] G. Krier, O. Jepsen, A. Burkhardt, O.K. Andersen, *The TB-LMTO-ASA program*, source code, version 4.7, available upon request from the program authors.

[21] B.I. Min, Y.-R. Jang, *J. Phys., Condens. Matter* **3,** 5131 (1991).

[22] U. von Barth, L. Hedin, *J. Phys. C* **5,** 1629 (1972).

[23] J.P. Perdew, J.A. Chevary, S.H. Vosko, K.A. Jackson, M.R. Pederson, D.J. Singh, C. Fiolhais, *Phys. Rev. B* **46,** 6671 (1992).

[24] O. Jepsen, O.K. Andersen, *Solid State Commun.* **9,** 1763 (1971).

[25] O. Jepsen, O.K. Andersen, *Phys. Rev. B* **29,** 5965 (1984).

[26] P. Blöchl, O. Jepsen, O.K. Andersen, *Phys. Rev. B* **49,** 16223 (1994).

[27] E. Gurewitz, H. Pinto, M. Dariel, H. Shaked, *J. Phys. F, Met. Phys.* **13,** 545 (1983).

[28] K. Hummler, M. Fähnle, *Phys. Rev. B* **53,** 3272 (1996).

[29] F.M. Mulder, R. Coehoorn, R.C. Thiel, K.H.J. Buschow, *Phys. Rev. B* **56,** 5786 (1997).

[30] V.V. Aleksandryan, K.P. Belov, P.Z. Levitin, A.S. Markosyan, W.W. Snegirev, *Pis'ma Zh. Eksp. Teor. Fiz.* **40,** 77 (1984).

[31] I. Shidlovsky, W.E. Wallace, *J. Solid State Chem.* **2,** 193 (1970).

[32] C.V. Thang, N.H. Duc, M.M. Tan, N.P. Thuy, E. Brück, P.E. Brommer, J.J.M. Franse, *J. Magn. Magn. Mater.* **177-181,** 819 (1998).

[33] K. Konno, H. Ido, S.F. Cheng, S.G. Sanker, W.E. Wallace, *J. Appl. Phys.* **73,** 5929 (1993).